Thermal Diffusivity of an Epoxy System as a Function of the Hardener Content

J. R. M. d'ALMEIDA,[1] N. CELLA,[2] S. N. MONTEIRO,[3] L. C. M. MIRANDA[4]

[1] Departamento de Ciência dos Materiais e Metalurgia, Pontificia Universidade Católica do Rio de Janeiro, 22453-900 Rio de Janeiro, RJ, Brazil

[2] Instituto Politécnico, Universidade do Estado do Rio de Janeiro, C.P. 97282, 28601-970 Nova Friburgo, RJ, Brazil

[3] Centro de Ciência e Tecnologia, Universidade Estadual do Norte Fluminense, 28015-820 Campos, RJ, Brazil

[4] Laboratório Associado de Sensores e Materiais, Instituto Nacional de Pesquisas Espaciais, 12201-970, São José dos Campos, SP, Brazil

Received 15 September 1997; accepted 6 December 1997

ABSTRACT: The influence on the thermal diffusivity of the changes induced on the macromolecular network of an epoxy-amine system by different hardener/resin ratios was experimentally investigated. For each hardener/resin ratio, the open photoacoustic cell technique was used to measure the thermal diffusivity. The thermal diffusivity data was correlated with the evolution of the characteristic infrared absorption bands of the epoxy and amine components using a fast Fourier transform spectrometer. The results show a sharp transition in the thermal diffusivity values at the beginning of the amine-rich domain, corresponding to a transformation from a rigid network to an amine saturated deformable structure. It is concluded that the open photoacoustic cell technique can be a useful monitoring tool for structural characterization and molecular evolution during the curing of this kind of system. © 1998 John Wiley & Sons, Inc. J Appl Polym Sci 69: 1335–1341, 1998

Key words: epoxy resin; thermal diffusivity; photoacoustic; open photoacoustic cell technique

INTRODUCTION

Epoxy resins are currently some of the most widely used thermoset polymers. Applications of these materials range from common to structural adhesives, as well as matrix materials, for high performance composites.[1,2] The outstanding versatility of this resin is basically due to the high reactivity of the epoxy group with different compounds like aliphatic and aromatic amines, anhydrides, and polyamides.[3] By selecting distinct types of hardeners, a large variety of epoxy systems can be produced with distinct mechanical, physical, and chemical properties. Besides the type of hardener used in the preparation of the epoxy system, the properties of the final macromolecular network are also strongly dependent upon the time and the temperature of curing.[4–6] Therefore, a comprehensive picture of the molecular changes that occur as a function of these processing parameters is of great value in understanding the resulting modifications of the final physical properties of epoxy based materials.

In this article we report on the changes of the

Correspondence to: J. R. M. d'Almeida (dalmeida@rdc.puc-rio.br).

Contract grant sponsor: CNPq and FAPERJ.

Journal of Applied Polymer Science, Vol. 69, 1335–1341 (1998)
 CCC 0021-8995/98/071335-07

Table I Infrared Relative Intensity of Epoxy Band at 916 cm^{-1} (I) and Degree of Cure of Epoxy Mixtures (α_c)

phr	$I = A_{916}/A_{806}$	α_c
0	20.05 ± 2.35	—
7	5.81 ± 1.25	0.71
9	4.65 ± 1.08	0.77
11	4.52 ± 0.96	0.77
13[a]	4.14 ± 0.61	0.79
15	3.20 ± 1.10	0.84
17	3.56 ± 1.23	0.82
19	1.29 ± 0.10	0.94
21	1.32 ± 1.30	0.93

[a] Stoichiometric ratio.

thermal diffusivity of an epoxy–aliphatic amine system as a function of the hardener/epoxy resin ratio. The thermal diffusivity is an important physical parameter that is strongly dependent on the compositional and microstructural variables' internal structure of the material,[7–9] as well as on the processing conditions.[10,11] The changes of the thermal diffusivity of our epoxy samples are compared to the corresponding changes observed in the infrared spectra and the thermogravimetric analysis.

EXPERIMENTAL

Sample Preparation

The samples were prepared by mixing proper quantities of a difunctional epoxy monomer, diglycidyl ether of bisphenol A (DGEBA), with an aliphatic amine, triethylene tetramine (TETA). Eight different hardener/resin ratios were prepared that covered the range of epoxy-rich to amine-rich compositions, including the stoichiometric one. The different hardener/resin ratios used in this work were labeled according to the amount of hardener in weight (per hundred parts of resin, phr) and are summarized in Table I. For the particular epoxy system investigated, the stoichiometric ratio corresponds to 13 phr. The cure of our samples was carried out at 25 ± 3°C.

Bulk and thin film specimens were prepared after thoroughly mixing the appropriate quantities of epoxy monomer and hardener, which were weighed within ±0.0002 g. With this accuracy we were able to produce samples with deviations in phr values smaller than 1.5%. The bulk samples were cast in bar-shaped open silicone molds. The samples had an average 16-mm^2 area and 150-μm thickness and were cut from the bar-shaped blocks using a low speed saw in the x, y, and z directions as schematically shown in Figure 1(a). The thin film samples were cast directly onto an aluminum foil substrate as indicated in Figure 1(b). A cardboard frame was glued to the aluminum substrate, and the resin mixture was poured into the window left by the frame. To insure uniform thickness, the resin was spread with the aid of a spatula. The thickness of these thin film samples ranged between 150 and 200 μm.

Infrared Spectroscopy

The degree of curing of our samples was evaluated by monitoring the changes of the epoxy ring infrared absorption band at 916 cm^{-1} using an FTIR spectrometer (Nicolet FTIR-520) with a resolu-

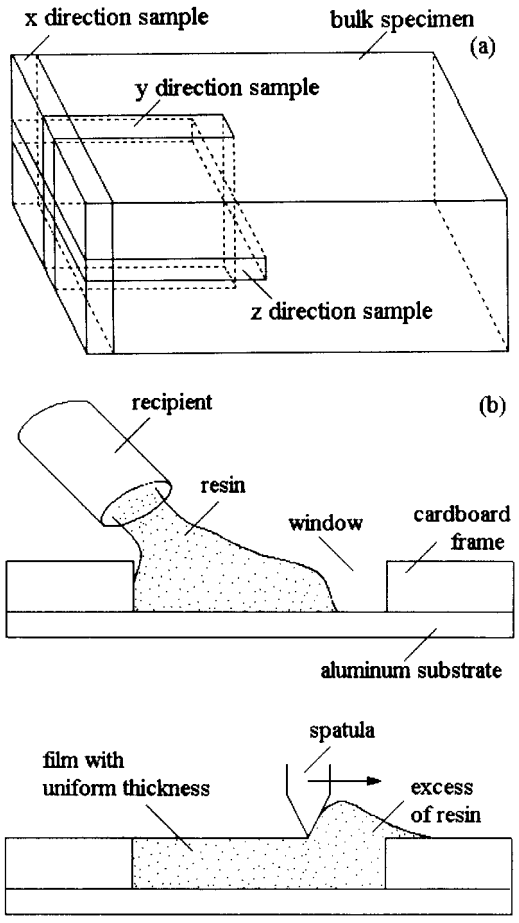

Figure 1 (a) The bulk specimen with the corresponding cutting axes. (b) Schematic procedure for the thin film sample fabrication.

tion of 2 cm^{-1}. Thin film samples and samples cut from the bulk specimen were analyzed. Eight different amine/epoxy mixtures were used in the investigation of the evolution of the 916-cm^{-1} band as a function of the hardener content. The 916-cm^{-1} line intensity was normalized with respect to the chemically unaffected phenyl group band at 806 cm^{-1}. The results obtained for the epoxy ring line intensity evolution are summarized in Table I.

Thermogravimetric Analysis

The thermogravimetric analysis (Perkin–Elmer series 7) was carried out using 3-mg samples. The temperature scanning ranged from 30 to 700°C at a heating rate of 10°C/min in an argon inert atmosphere.

Thermal Diffusivity

The thermal diffusivity, α, measures the rate of heat diffusion in a sample. It is defined by

$$\alpha = \kappa/\rho c \qquad (1)$$

where κ is the thermal conductivity, ρ is the density, and c is the heat capacity at constant pressure. The thermal diffusivities of a wide range of materials, such as polymers,[12] glasses,[13] and plant leaves,[14,15] can be accurately measured by the photoacoustic (PA) techniques.[16] The PA technique looks directly at the heat generated in a sample (due to nonradiative deexcitation processes) following the absorption of light (e.g., a fraction of the absorbed energy is converted to phonons or heat energy).[17,18] In the conventional PA experimental arrangement a sample enclosed in an air-tight cell is exposed to a chopped light beam. As a result of the periodic heating of the sample, the pressure in the chamber oscillates at the chopping frequency and can be detected by a sensitive microphone coupled to the cell. The resulting PA signal depends not only on the amount of heat generated in the sample (i.e., on the optical absorption coefficient and the sample light-into-heat conversion efficiency), but also on how the heat diffuses through the sample.

Of the existing PA techniques for the measurement of thermal diffusivity, we resorted to the so-called open photoacoustic cell (OPC) technique.[19,20] It consists of mounting the sample directly onto a cylindrical electret microphone as schematically shown in Figure 2. The typical design of an electret microphone consists of a metallized electret diaphragm (12 μm thick Teflon foil with metal coated electrodes) and a metal backplate separated from the diaphragm by a 45 μm long air gap. The top metal electrode and the backplate are connected through a resistor R. The front sound inlet is a circular hole of 3 mm diameter, and the front air chamber adjacent to the front face of the diaphragm is roughly 1 mm long. As a result of the periodic heating of the sample by the absorption of modulated light, the pressure in the front chamber oscillates at the chopping frequency, causing diaphragm deflections, which generates a voltage across the resistor R. This voltage is subsequently fed into a lock-in amplifier in which the amplitude and phase of the corresponding signal are analyzed.

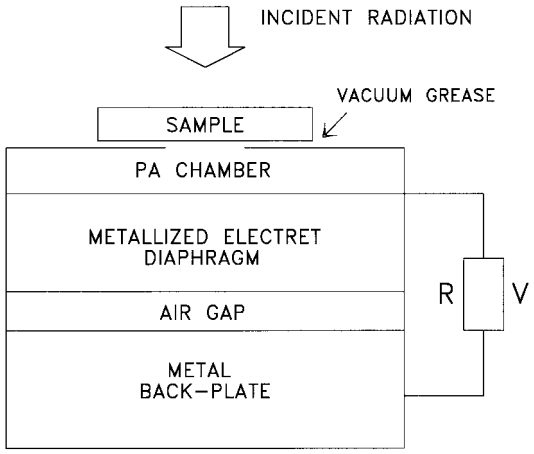

Figure 2 Schematic cross section of the open photoacoustic setup.

The general expression for the OPC signal is quite complicated, and we refer to the literature[14,16,19,20] for a detailed discussion of the OPC signal generation. It can be shown, however, that for a thermally thick and optically opaque sample, the OPC signal, V_{OPC}, can be written as[14]

$$V_{OPC} = (A/f)\exp(-a\sqrt{f}) \qquad (2)$$

where A is an overall scaling factor for the OPC signal independent of the modulation frequency, f, and a is given by

$$a = (\pi l^2/\alpha)^{1/2} \qquad (3)$$

where l represents the sample thickness. It follows from eqs. (2) and (3) that the sample's ther-

mal diffusivity α is obtained from the OPC signal data fitting (as a function of the modulation frequency) from the coefficient a given by eq. (3). The implicit optical opaqueness condition, meaning that all the incident radiation is fully absorbed at the front sample surface, was ensured by using a thin (12 μm thick) Al foil glued to the sample surface using a very thin layer of thermal paste. In Figure 3 we show a typical modulation frequency dependence of the OPC signal for a thin film sample (170 ± 5 μm thick) with 15 phr. The solid line in this figure corresponds to the best fit data using eq. (2). The corresponding value of the thermal diffusivity was 0.0023 cm^2/s.

RESULTS AND DISCUSSIONS

The degree of cure, α_c, obtained from the infrared data for the eight different phr resin mixtures, was calculated from the relationship[21]

$$\alpha_c = (I_0 - I)/I_0 \qquad (4)$$

where I denotes the epoxy band intensity for a given phr ratio and I_0 is the epoxy band intensity of the bare resin. The corresponding results are shown in Table I; in Figure 4 presents the plot of α_c as a function of the phr. Figure 4 tell us that the consumption of the epoxy rings, as measured by the degree of cure, increases monotonically with increasing values of phr. It can also be seen

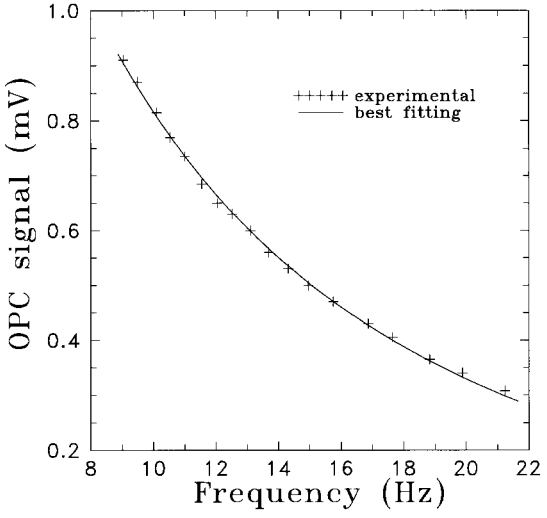

Figure 3 OPC signal amplitude as a function of the modulation frequency for a 170 ± 5 μm thick thin sample with 15 phr.

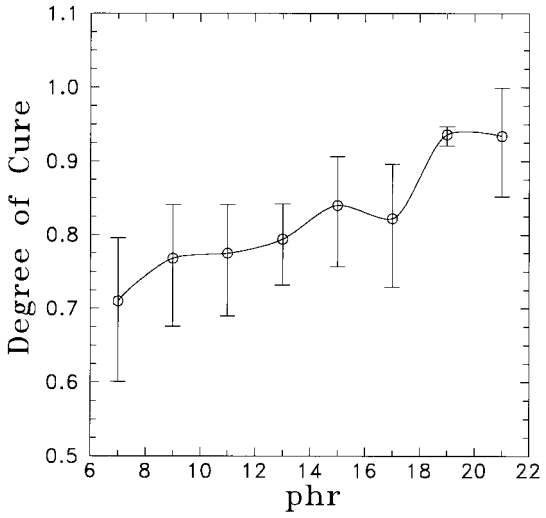

Figure 4 Degree of cure as a function of the (phr) as obtained from eq. (4) of the text.

that a small peak occurs at 15 phr, which is followed by a sudden jump above 17 phr. As shown in Figure 4, large error bars were found for all phr values except for 19 phr. All the data were obtained using the same experimental procedures. At least five FTIR scans were performed on different regions of each sample for the eight phr mixtures analyzed. Therefore, the source of the very low error bar associated with the 19 phr point was not clearly detected. Nevertheless, one could correlate the small error bar with the development of an homogeneous structure for that particular phr mixture.

The thermal diffusivity data obtained using the OPC technique for the different sample compositions are presented in Figures 5 and 6. Figure 5 shows the data from the thin film samples cast on an aluminum substrate and samples along the x direction that were taken from the region near the border of the bar-shaped bulk material [cf. Fig. 1(a)]. Figure 6 corresponds to samples along the y and z directions that were taken from the inner parts of the bulk material. The first point that attracts our attention is the fact that there is an apparent anisotropy in the thermal diffusivity of these samples. Furthermore, these features are more evident and exhibit a somewhat logical trend only in the amine-rich region corresponding to $>$ 13 phr. Accordingly, we restrict our discussion to this region of phr values. The data in Figure 6 exhibit, at least qualitatively, quite similar trends, especially in the amine-rich region of $>$ 13 phr. In contrast, both the x direction and the thin film samples (Fig. 5) exhibit quite similar

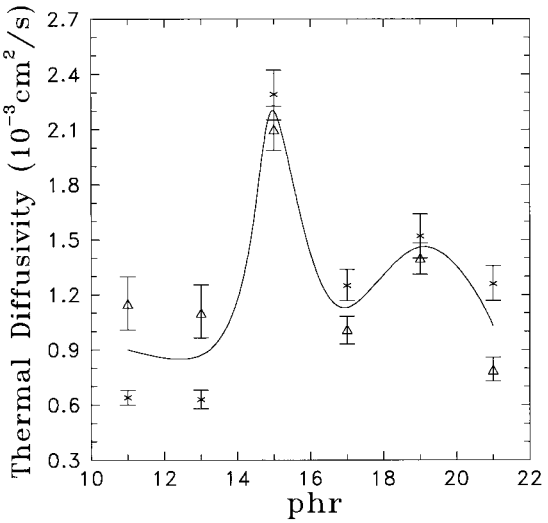

Figure 5 Thermal diffusivity as a function of the phr corresponding to samples cut along the (△) x and (×) for the thin film samples cast on an aluminum substrate. The solid curve represents a polynomial fitting through the mean data points of these two samples.

dependence on the phr, again in the amine-rich region. The behavior of the thermal diffusivity of the thin film and the x direction samples is, however, quite distinct from those of the y and z direction samples. The thin film and the x direction samples exhibit two marked peaks at 15 and 19 phr, whereas the y and z direction samples exhibit just a single peak at 15 phr. In fact, at 19 phr the thermal diffusivity of these last samples passes through a minimum in contrast to the thin film and the x direction samples that exhibit a peak at this phr.

The second interesting aspect worth mentioning regards the thermal diffusivity behavior at the stoichiometric point at 13 phr. This point corresponds, in principle, to the point at which all the epoxy rings would be consumed. For all samples studied, the stoichiometric point corresponds to the point at which the thermal diffusivity passed through a valley in the α versus phr. Furthermore, the data of the degree of cure summarized in Table I and plotted in Figure 4 show that the epoxy rings are almost totally consumed only for the amine-rich mixtures with 19 and 21 phr. This behavior may be attributed to the relatively fast liquid to gel transformation that occurs during the exothermic reaction in the amine-epoxy system. As the mobility of the chemical species is reduced in the course of the curing reaction, many epoxy rings remain unreacted, even with excess hardener. Furthermore, for $>$ 13 phr it is also possible that some of the reactivity points at the hardener molecules also remain unreacted.[22] This may be due to either the exhaustion of the epoxy groups[22] or to steric restrictions.[23] For the particular system studied, a strong transition in the mechanical properties was observed[24] between the epoxy-rich and the amine-rich mixtures. The mechanical behavior reported elsewhere[24] showed a marked change from a rigid macromolecular network to an amine saturated deformable structure. This behavior was attributed to the presence of unreacted sites of the hardener molecules.[25]

The data shown in Figures 5 and 6 also suggest that the changes introduced in the crosslinked network as the hardener content is increased is such that a sharp transition in the sample's thermal diffusivity is produced as we go from the epoxy-rich to the amine-rich domain at 15 phr. Coincidentally, the α_c data shown in Figure 4 also exhibits a peak at this 15 phr value. This closely correlated behavior of α and α_c as a function of the phr is more evident when comparing Figures 4 and 5, corresponding to the thermal diffusivity of the thin film samples. Both figures exhibit sharp transitions at 15 and 19 phr values. The peaks observed in the thermal diffusivity of the thin film samples as depicted in Figure 5 indicate that more organized structures are being formed at these values of phr. This is physically expected from eq. (1) by remembering that more organized

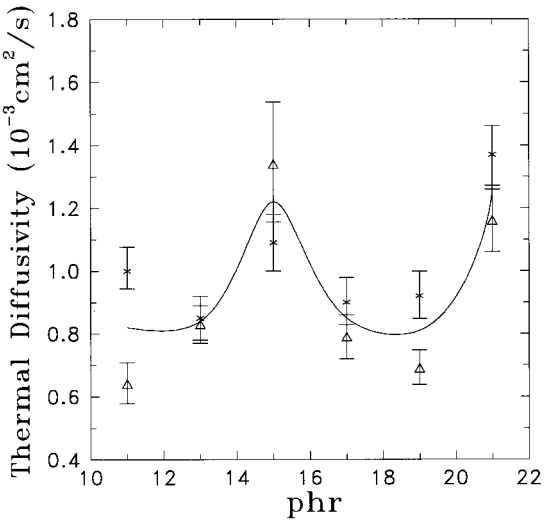

Figure 6 Thermal diffusivity as a function of the phr corresponding to samples cut along the (×) y and (△) z directions. The solid curve represents a polynomial fitting through the mean data points of these two samples.

structures have higher thermal conductivity than those of less organized ones. In fact, this hypothesis of structural changes taking place in our samples with increasing hardener content is quite evident in the thermogravimetric analysis. In Figure 7(a–d) we present the results of the thermogravimetric analysis corresponding to 13, 15, 17, and 21 phr, respectively. For 13 phr, the spectrum in Figure 7(a) exhibits just a single sharp peak centered around 375°C, corresponding to a relatively uniform distribution of crosslinks. For 15 phr, the spectrum changes to a broad peak at around 375°C with smaller side bands, indicating a two phase system in which one has a dispersed phase of a rigid network embedded in a matrix of uniform density. In Figure 7(c) the thermogravimetric spectrum corresponding to 17 phr becomes quite similar to that of 13 phr, consisting of a single sharp peak. For 21 phr, the spectrum shown in Figure 7(d) exhibits again a broad peak at around 375°C with two maxima, indicating that the system consists of a two phase network. We note that the 13 and 17 phr correspond to the points at which the thermal diffusivity data shown in Figure 5 exhibit a valley.

Finally, we address the different behavior of the thermal diffusivity between the x direction and the thin film sample and the y and z direction samples. The results in Figure 5, with the two peaks at 15 and 19 phr, suggest that two microstructures are present in the thin filmlike samples. In contrast, for samples taken from the bulk (cf. Fig. 6), the thermal diffusivity exhibits just a single peak corresponding to just one kind of microstructure. In other words, these results suggest that in the thin filmlike samples, one may have two distinct distributions of particle aggregates in our system, whereas for the bulk samples just a single average aggregate is formed. Many parameters, such as the substrate (aluminum foil for the thin film samples and the silicone wall for the x direction samples) and the cure temperature,[26] may be responsible for that. Near the border or in the thin film sample grown on the Al substrate, the local interface temperature is smaller than in the bulk due to higher thermal conductance to the substrate (i.e., the substrate acts as a heat sink). On the other hand, small temperatures favor[26] the formation of larger size aggregates. As one increases the hardener content, the local temperature increases due to the exothermic nature of the curing reaction so that small density particles are expected to be formed. In the case of the bulk samples there should be

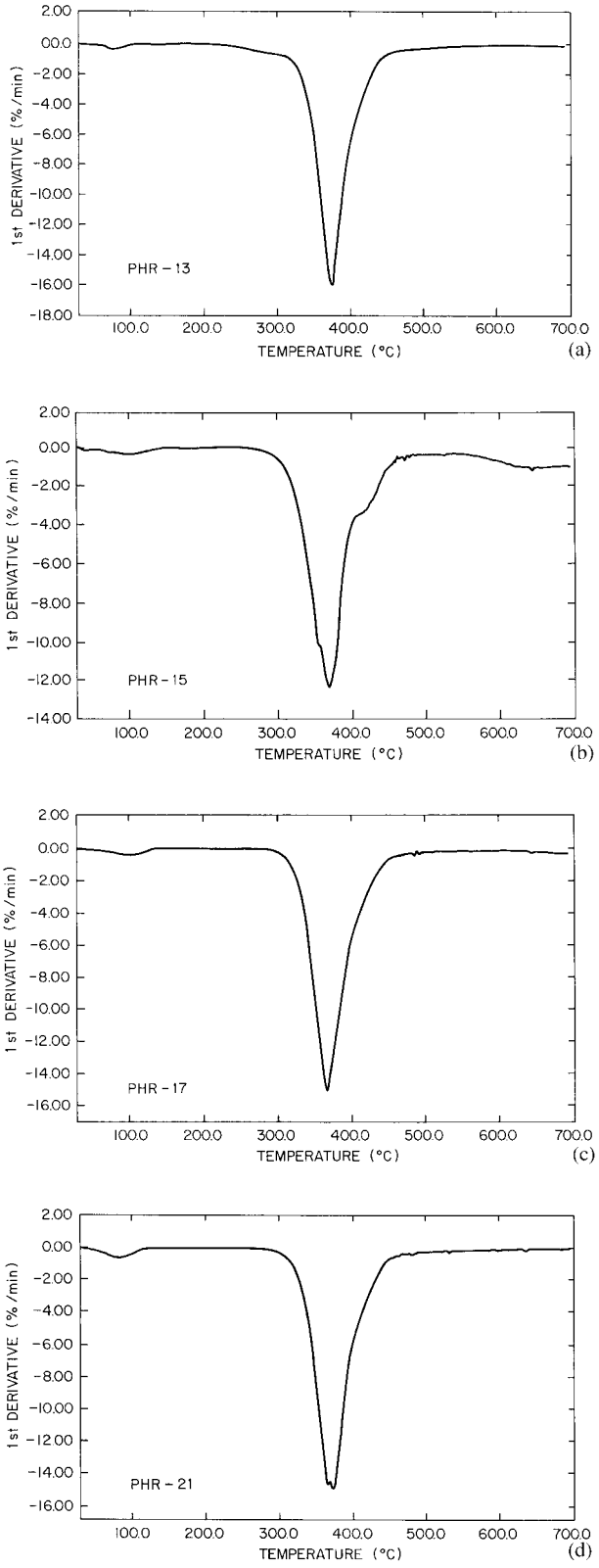

Figure 7 Thermogravimetric weight loss derivative as a function of temperature for samples with (a) 13, (b) 15, (c) 17, and (d) 21 phr.

no significant change of temperature due to the larger heat bath, so just a single phase of particles is expected to be formed.

CONCLUSIONS

In this study we investigated the changes induced in the thermal diffusivity of an TETA/DGEBA epoxy system as a function of the hardener content. As expected, the changes of the thermal diffusivity reflected the structural changes that took place in the macromolecular network as a function of the amine content. Two marked behaviors were found for the thermal diffusivity of the thin film and bulk samples. This distinct behavior was speculatively explained as being due to distinct phases that may be formed in the system as a function of the local curing temperature at the interface and in the bulk.

Even though more detailed studies are needed for a more conclusive model explaining the differences in the thermal diffusivity reported in this article, we believe that we have demonstrated the usefulness of the OPC technique as a powerful tool for the thermal characterization of curing processes and polymer processing in general.

This work was partially financed by the Brazilian Agencies CNPq and FAPERJ whose support is greatly appreciated.

REFERENCES

1. J. M. Margolis, *Advanced Thermoset Composites—Industrial and Commercial Applications,* Van Nostrand Reinhold Co., New York, 1985.
2. R. S. Bauer and L. S. Corley, in *Reference Book for Composites Technology,* Vol. 1, S. M. Lee, Ed., Technomic Publ. Co., Lancaster, PA, 1989, p. 17.
3. H. Lee and K. Neville, *Handbook of Epoxy Resins,* McGraw–Hill, New York, 1967.
4. S. Yamini and R. J. Yong, *J. Mater. Sci.,* **14,** 1609 (1979).
5. J. Tang and G. S. Springer, *J. Compos. Mater.,* **22,** 2 (1988).
6. R. J. Morgan and E. T. Mones, *J. Appl. Polym. Sci.,* **33,** 999 (1987).
7. G. Ziegler and D. P. H. Hasselman, *J. Mater. Sci.,* **16,** 495 (1981).
8. N. F. Leite, A. H. Franzan, A. Torres–Filho, and L. C. M. Miranda, *J. Appl. Polym. Sci.,* **39,** 1361 (1990).
9. N. F. Leite and L. C. M. Miranda, *J. Mater. Sci.,* **27,** 5449 (1992).
10. A. Torres–Filho, L. F. Perondi, and L. C. M. Miranda, *J. Appl. Polym. Sci.,* **35,** 103 (1988).
11. A. H. Franzan, N. F. Leite, and L. C. M. Miranda, *Appl. Phys.,* **A50,** 431 (1990).
12. A. Torres–Filho, N. F. Leite, L. C. M. Miranda, N. Cella, and H. Vargas, *J. Appl. Phys.,* **66,** 97 (1989).
13. J. C. Lima, N. Cella, L. C. M. Miranda, C. Chying An, A. H. Franzan, and N. F. Leite, *Phys. Rev.,* **B46,** 14186 (1992).
14. M. V. Marquezini, N. Cella, A. M. Mansanares, H. Vargas, and L. C. M. Miranda, *Meas. Sci. Technol.,* **2,** 396 (1991).
15. A. C. Pereira, M. Zerbetto, G. C. Silva, H. Vargas, W. J. Silva, G. O. Neto, N. Cella, and L. C. M. Miranda, *Meas. Sci. Technol.,* **3,** 931 (1992).
16. H. Vargas and L. C. M. Miranda, *Phys. Rep.,* **161,** 45 (1988).
17. A. Rosencwaig, *Science,* **181,** 657 (1973).
18. A. Rosencwaig and A. Gersho, *J. Appl. Phys.,* **47,** 64 (1976).
19. M. D. Silva, I. N. Bandeira, and L. C. M. Miranda, *J. Phys. E: Sci. Instrum.,* **20,** 1476 (1987).
20. L. F. Perondi and L. C. M. Miranda, *J. Appl. Phys.,* **62,** 2955 (1987).
21. W. Wu, D. L. Hunston, H. Yang, and R. S. Stein, *Macromolecules,* **21,** 756 (1988).
22. A. Gross, H. Brockmann, and H. Kollek, *Int. J. Adhesion Adhesives,* **7,** 33 (1987).
23. S. S. Yoon, W. J. Yu, and H. C. Kim, *J. Mater. Sci. Lett.,* **11,** 1392 (1992).
24. J. R. M. d'Almeida and S. N. Monteiro, *Pol. Testing,* **15,** 329 (1996).
25. E. Cuddihy and J. Moacanin, in Advances in Chemistry Series, 92, American Chemical Society, Washington, D.C., 1970, Chap. 9.
26. R. E. Cuthrell, *J. Appl. Polym. Sci.,* **11,** 949 (1967).